Discrete least square method (DLSM) for the solution of free surface seepage problem

Ali Rahmani Firoozjaee[1], **Mohammad Hadi Afshar**[2]

[1]PhD. student, civil engineering department, university of science and technology, Tehran, Iran
[2]Assistant professor, civil engineering department, university of science and technology, Tehran, Iran

Abstract: *A meshless method namely, discrete least square method (DLSM), is presented in the paper for the solution of free surface seepage problem. In this method computational domain is discredited by some nodes and then the set of simultaneous equations are built using moving least square (MLS) shape functions and least square technique. The proposed method does not need any background mesh therefore it is a truly meshless method. Several numerical two dimensional examples of Poisson partial differential equations (PDEs) are presented to illustrate the performance of the present DLSM. And finally a free surface seepage problem in a porous media is solved and results are presented.*

Keywords: *Numerical analysis, Meshless method, MLS, Least square technique, Poisson PDE, Seepage problem, DLSM*

Introduction

Over the last decade, meshless methods for the solution of partial differential equations (PDEs) have become increasingly popular. The main idea of these methods is to approximate the unknown field by a linear combination of shape functions built without having recourse to a mesh of the domain. Instead, nodes are scattered in the domain and a certain weight function with a local support is associated with each of these nodes. The shape function associated with a given node is then built considering the weight functions whose support overlaps the one of the weight function of this node; thus, there is actually no need to establish connectivities between the different nodes as in the finite element method. Although the construction of the shape functions is more expensive for meshless methods than for the latter one, they are prime methods for problems with moving boundaries because no remeshing of the domain is necessary.

In order to overcome the disadvantages of mesh-based numerical methods, such as the finite element method (FEM), various meshless methods have been developed and successfully used in solving problems governed by ordinary differential equations (ODEs) or partial differential equations (PDEs). The meshless methods have been developed in recent years are smooth particle hydrodynamics (SPH) [1], the element free Galerkin (EFG) method[2,3], the reproducing kernel particle (RKP) method[4], the finite point (FP) method[5], the hp clouds method[6], meshless local Petrov-Galerkin (MLPG) method[7-10], local boundary integral equation (LBIE)method[8-12], least square collocation meshless (LSCM) method[13], point weighted least square (PWLS) method[14].

In this research a meshless method namely, discrete least square method (DLSM), is proposed. In this method computational domain is discretized by some nodes and then the set of simultaneous equations are built using moving least square (MLS) shape

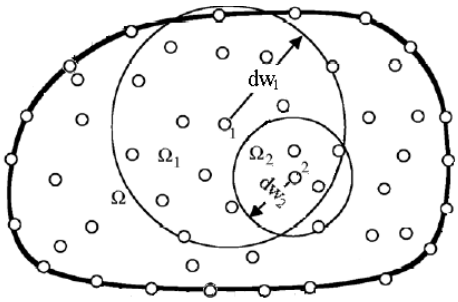

Fig.1. Schematic presentation of influence domain of 2 nodes

functions and least square technique. The presented method does not need any background mesh therefore it is a truly meshless method and the stiffness matrix is symmetric. In section 2 constructing of moving least square is explained, in section 3 Discrete least square method (DLSM) (for disretization) is elaborated. At last a numerical example and a seepage problem are solved by this approach.

Moving least square shape functions

The most frequently used approximation in meshless methods is the moving least squares interpolant in which the unknown function ϕ is approximated by:

$$\phi(X) = \sum_{i=1}^{m} p_i(X)a_i(X) = P^T(X)a(X) \quad (1)$$

Where $P^T(X)$ is a polynomial basis in the space coordinates, and m is the total number of the terms in the basis. For a 2D problem we can specify $P=[1\ x\ y\ x^2\ xy\ y^2]$ for $m=6$. $a(x)$ is the vector of coefficients is and can be obtained by minimizing a weighted discrete L_2 norm as follows:

$$J = \sum_{i=1}^{n} w_j(X - X_J)(P^T(X_j)a(X) - u_j^h)^2 \quad (2)$$

Where $w_j(X - X_j)$ is the weight function and u_j^h is the value of the nodal parameters at node j. $w_j(X - X_j)$ is built in such a way that vanishes outside a region Ω_j surrounding the point j. This local domain is termed as influence domain of node j. Influence domain can have different shapes and sizes and its size can be different for different nodes as illustrated in Fig. (1). In this study circular influence domain with radius dw_j and cubic spline weight function is considered as defined by Eq. (3):

$$w(X - X_j) = w(\bar{d}) = \begin{cases} \frac{2}{3} - 4\bar{d}^2 + 4\bar{d}^3 & \text{for } \bar{d} \le \frac{1}{2} \\ \frac{4}{3} - 4\bar{d} + 4\bar{d}^2 - \frac{4}{3}\bar{d}^3 & \text{for } \frac{1}{2} \le \bar{d} \le 1 \\ 0 & \text{for } \bar{d} > 1 \end{cases} \quad (3)$$

Where $\bar{d} = ||X\text{-}X_j||/d_w$ and d_w is the size of influence domain of node j.

Minimization of equation (2) leads to

$$\phi(X) = P^T(X)A^{-1}(X)B(X)\phi^h \quad (4)$$

where

$$A(X) = \sum_{j=1}^{n} w_j(X - X_j)P(X_j)P^T(X_j) \quad (5)$$

$$B(X) = [w_1(X\text{-}X_1)P(X_1),\ w_2(X\text{-}X_2)P(X_2),\ \ldots,\ w_n(X\text{-}X_n)P(X_n)] \quad (6)$$

Comparing equation (4) with the well known form of equation (7) yields to equation (8)

$$\phi(X) = N^T(X)\phi^h \tag{7}$$

$$N^T(X) = P^T(X)A^{-1}(X)B(X) \tag{8}$$

$N^T(X)$ contains the shape functions of nodes at point (X) witch are called moving least square (MLS) shape functions.

Discrete least square method (DLSM)

Consider the following (partial) differential equation

$$A(\phi) + f = 0 \text{ in } \Omega \tag{9}$$

subject to appropriate Drichlet and Neuman boundaries.

$$\phi - \bar{\phi} = 0 \text{ on } \Gamma_2 \tag{10}$$

$$B(\phi) - \bar{t} = 0 \text{ on } \Gamma_1 \tag{11}$$

Where A, B are (partial) differential operators, and f represents external forces or source term on the problem domain.
Upon disretization of the problem domain and its boundaries using Equation (7) defined as the residual of partial differential equation at a typical node k is:

$$\begin{aligned} R_\Omega(x_k) &= A(\phi(x_k)) + f(x_k) \\ &= \sum_{j=1}^{n} A(N_j(x_k))\phi_j + f(x_k) \quad , \quad k = 1, n \end{aligned} \tag{12}$$

As discrete least square method uses strong formulation, to satisfy Neuman boundary condition a penalty formulation is required. The residual of Neuman boundary condition at typical node k on the Neuman boundary can be written as:

$$R_1(x_k) = B(\phi) - \bar{t}(x_k) = \sum_{j=1}^{n} B(N_j(x_k))\phi_j - \bar{t}(x_k)$$
$$, \quad k = 1, n_1 \tag{13}$$

and finally as moving least square (MLS) shape functions do not enjoy Kronecker Delta property, to satisfy Drichlet boundary condition a penalty formulation is required. The residual of Drichlet boundary condition at nodes on the Drichlet boundary could be stated by:

$$R_2(x_k) = \phi - \bar{\phi}(x_k) = \sum_{j=1}^{n} N_j(x_k)\phi_j - \bar{\phi}(x_k)$$
$$, \quad k = 1, n_2 \tag{14}$$

where n is the total number of nodes and n_1 and n_2 are the number of nodes on Drichlet and neuman boundaries respectively. A penalty approach is used to form the total residual of the problem defined as:

$$I = \sum_{k=1}^{n} (R_\Omega^2(x_k) + \alpha_1 R_1^2(x_k) + \alpha_2 R_2^2(x_k)) \tag{15}$$

$$I = \sum_{k=1}^{n} R_\Omega^2(x_k) + \alpha_1 \sum_{k=1}^{n} R_1^2(x_k) + \alpha_2 \sum_{k=1}^{n} R_2^2(x_k) \tag{16}$$

$$\begin{aligned} I &= \sum_{k=1}^{n}\sum_{j=1}^{n} \left[A(N_j(x_k))\phi_j + f(x_k)\right]^2 \\ &+ \alpha_1 \sum_{k=1}^{n}\sum_{j=1}^{n} \left[B(N_j(x_k))\phi_j - \bar{t}(x_k)\right]^2 \\ &+ \alpha_2 \sum_{k=1}^{n}\sum_{j=1}^{n} \left[N_j(x_k)\phi_j - \bar{\phi}(x_k)\right]^2 \end{aligned} \tag{17}$$

where α_2 and α_1 are penalty coefficient for Drichlet and Neuman boundary conditions respectively. Minimization of the functional with respect to nodal parameters (ϕ_i , $i=1,2,...,n$) leads to the following system of equations.

$$K\phi = F \tag{18}$$

where

$$\begin{aligned} K_{ij} &= \sum_{k=1}^{n} A(N_i(x_k))A(N_j(x_k)) \\ &+ \alpha_1 \sum_{k=1}^{n} B(N_i(x_k))B(N_j(x_k)) \end{aligned} \tag{19}$$

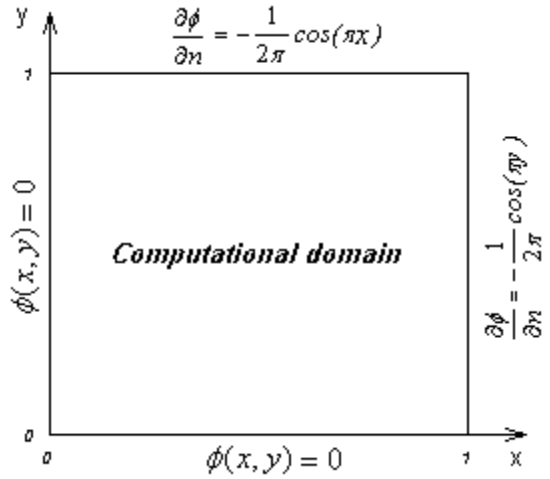

Fig.2. Computational domain and boundary condition of example 1.

$$F_i = -\sum_{k=1}^{n} A(N_i(x_k))f(x_k) + \alpha_1 \sum_{k=1}^{n} B(N_i(x_k))\bar{t}(x_k) + \alpha_2 \sum_{k=1}^{n} N_i(x_k)\bar{\phi}(x_k) \quad (20)$$

the system of equations is clearly allowing for efficient solvers to be used.

Numerical examples

To illustrate the accuracy and efficiency of the proposed method, some two dimensional numerical examples are considered. In all the examples P is considered as $P = [1 \ x \ y \ x^2 \ xy \ y^2]$ and the dw for each node is calculated in such a way that each point is supported by at least 20 nodes.

1. 2D Poisson partial differential Equation

Consider the 2D Poisson equation defined in a square domain which is taken from [14]:

$$\frac{\partial^2 \phi}{\partial x^2} + \frac{\partial^2 \phi}{\partial y^2} = \sin(\pi x)\sin(\pi y) \ , 0 \leq x, y \leq 1 \quad (21)$$

With the following Drichlet and Neumn boundary condition

$$\phi(x, y)\big|_{x=0} = 0 \qquad \phi(x, y)\big|_{y=0} = 0 \quad (22)$$

$$\left.\frac{\partial \phi}{\partial x}\right|_{x=1} = -\frac{1}{2\pi}\cos(\pi y) \qquad \left.\frac{\partial \phi}{\partial y}\right|_{y=1} = -\frac{1}{2\pi}\cos(\pi x) \quad (23)$$

Computational domain and boundary conditions are illustrated in Fig. (2). The exact solution of this problem can be easily obtained

$$\phi^{exact} = -\frac{1}{2\pi}\sin(\pi x)\sin(\pi y)$$

The problem is discretized in 2 models. One is 121 nodes distributed regularly in problem domain and the other is 228 irregular nodes generated by random.

Following error norms are defined as error indicators in this paper:

$$e_{\circ} = \frac{1}{N}\frac{\sum_{i=1}^{N}\left|u_i^{exact} - u_i^{num}\right|}{\sum_{i=1}^{N}\left|u_i^{exact}\right|} \quad (24)$$

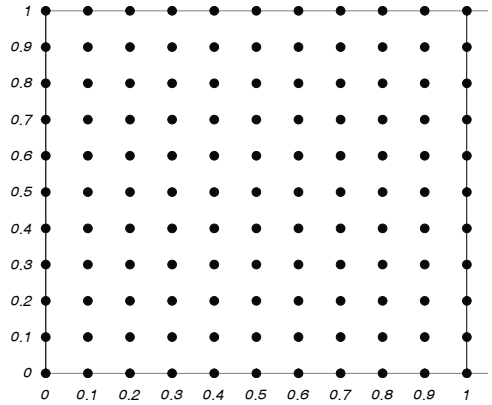

Fig.3. regularly nodes in problem domain

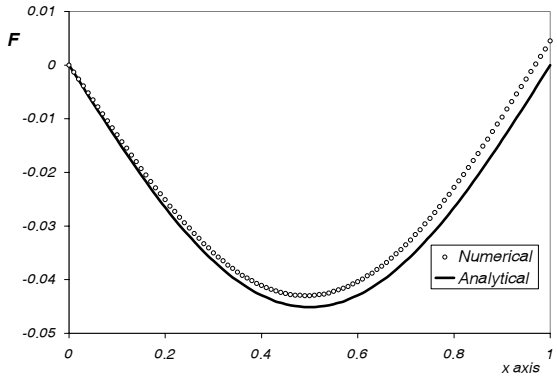

Fig.4. exact and numerical solution at y=0.35

$$e_{1x} = \frac{1}{N} \frac{\sum_{i=1}^{N} \left| u_{i,x}^{exact} - u_{i,x}^{num} \right|}{\sum_{i=1}^{N} \left| u_{i,x}^{exact} \right|} \tag{25}$$

$$e_{1y} = \frac{1}{N} \frac{\sum_{i=1}^{N} \left| u_{i,y}^{exact} - u_{i,y}^{num} \right|}{\sum_{i=1}^{N} \left| u_{i,y}^{exact} \right|} \tag{26}$$

In which u_i^{exact} and u_i^{num} are the exact solution and the numerical solution of the function at node *i*, respectively. $u_{i,x}$ and $u_{i,y}$ are derivatives respect to *x* and *y*, *N* is the number of nodes.

1.1 121 regular nodes

The computational domain illustrated in Fig. (2) is discretized using 121 regularly distributed nodes and the position of the

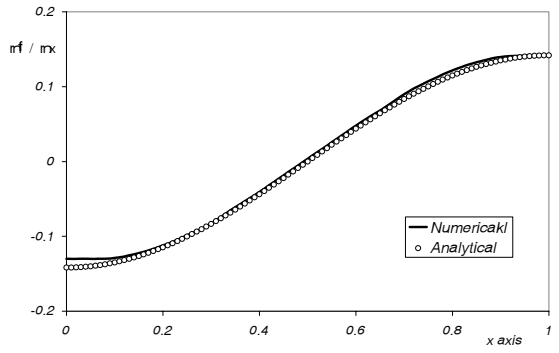

Fig.5. exact & approximated $\partial\phi/\partial x$ at y=0.35

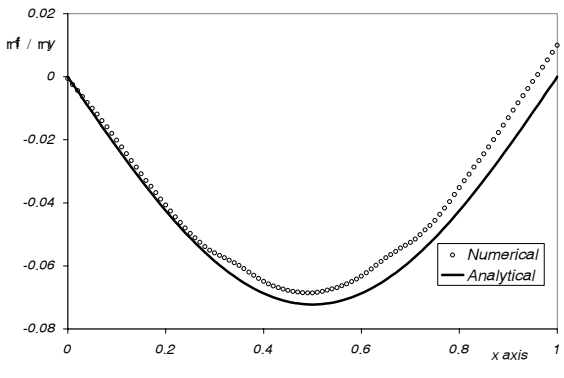

Fig.6. exact & approximated $\partial\phi/\partial y$ at y=0.35

nodes are illustrated in figure (3). For comparison the approximated solution and exact solution at *y=0.35* are presented in figure (4), in figures (5) and (6) approximated derivatives respect to *x* and *y* are compared with their exact solutions.

as shown in figures (4) to (6) the approximation for 121 uniformly nodes are acceptable. By using equations (24) to (26) error norms are calculated (0.0014422), (0.0082645) and (0.0082645) for the solution and derivative of the solution respect to *x* and *y* respectively.

Table 1 sensitivity analysis on the number of nodes

N	Δx	e_0	e_{1x}	e_{1y}
36	0.2	0.013178	0.027778	0.027778
121	0.1	0.001442	0.008265	0.008265
441	0.05	0.000133	0.002268	0.002268

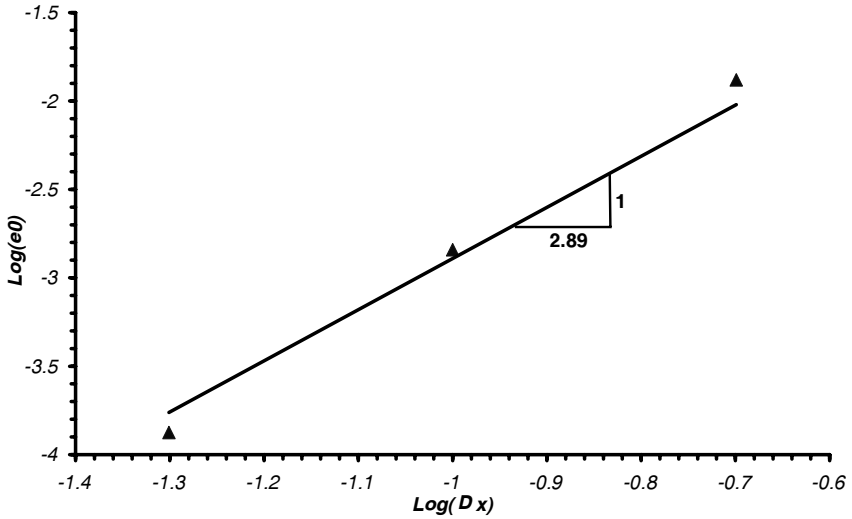

Fig.7. Convergence rate with a complete second order

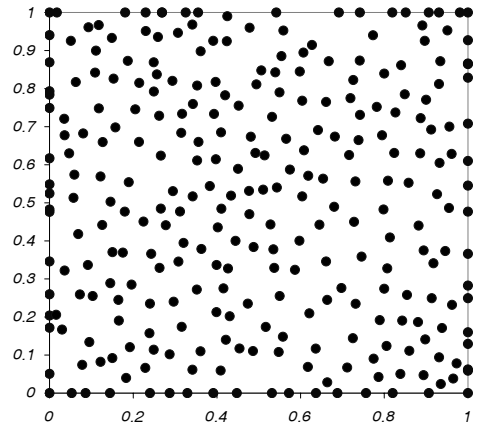

Fig.8. irregularly distributed nodes in domain

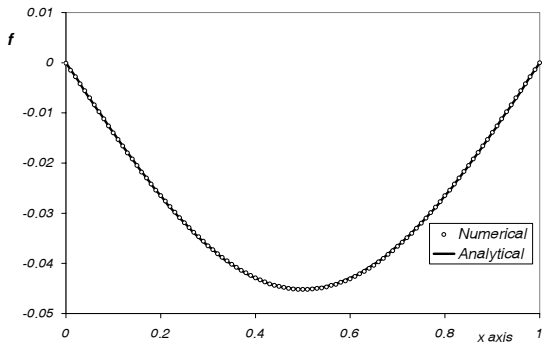

Fig.9. exact and approximated solution at y=0.35

Sensitivity analysis is done on the number of nodes. In this cases 36 nodes, 121 nodes and 441 nodes are considered, results are presented in table (1) and convergence rate is illustrated in figure (7).

1.2 282 irregular nodes

The above mentioned partial differential equation (Eqs. 21-23) is solved using 282 irregularly distributed nodes to discretize the computational domain and node positioning is illustrated in figure (8). For comparison the approximated solution and exact solution at *y= 0.35* are presented in figure (9), in figures (10) and (11) approximated derivatives respect to *x* and *y* are compared with their exact solutions.

2. Seepage problem

A typical problem of the flow through a homogenous earthfill dam is considered here as shown in figure 10. Dam's height is 25 meters, upstream water height is 22 meters and crest width is 3 meters. Problem domain is discretized by 139 nodes in which 70 nodes are on the boundaries. First iteration disretization is presented in Fig. (12). The governing partial differential equation is

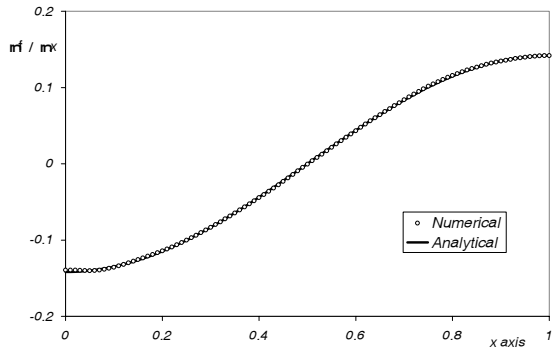

Fig.10. exact & approximated $\partial\phi/\partial x$ at y=0.35

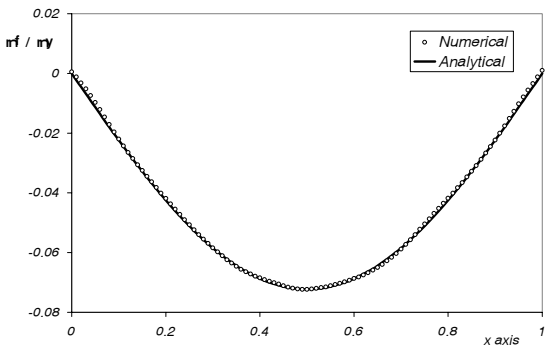

Fig.11. exact & approximated $\partial\phi/\partial y$ at y=0.35

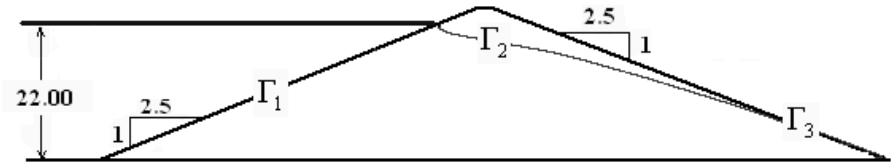

Fig.12. earthfill dam and its boundaries

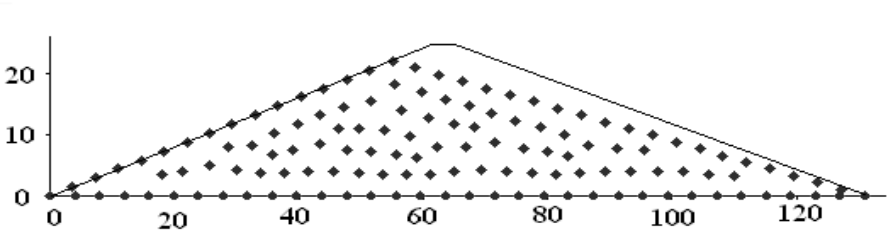

Fig.13. 139 nodes to discretized the problem domain

Laplace partial differential:

$$\frac{\partial^2\phi}{\partial x^2}+\frac{\partial^2\phi}{\partial y^2}=0. \qquad (29)$$

and boundary conditions are as follow:

$$\begin{array}{ll} \phi = 22\ m & on\ \Gamma_1 \\ \partial\phi/\partial n = 0\ \ and\ \ \phi = y & on\ \Gamma_2 \\ \phi = y & on\ \Gamma_3 \\ \partial\phi/\partial n = 0 & on\ \Gamma_4 \end{array} \qquad (30)$$

Γ_2 and Γ_3 are not known a prior and should, therefore, be obtained during the solution of the problem. A common procedure to solve this problem is an iterative method in which the boundaries Γ_2 and Γ_3 are initially guessed. With the boundary of the problem domain defined, the resulting seepage problem with Neuman boundary condition on Γ_2 is then solved to get the potentials at all nodal points including the point used to

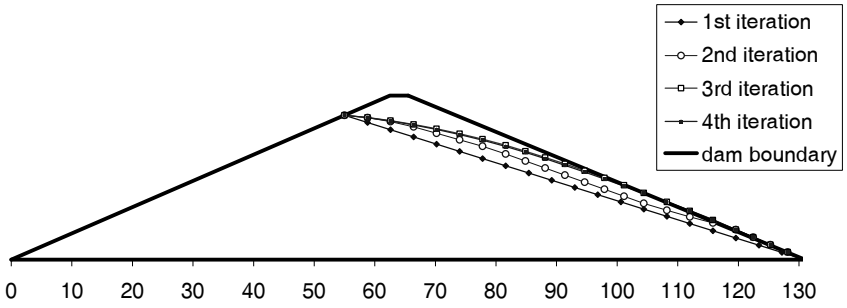

Fig.14. free surface for each iteration

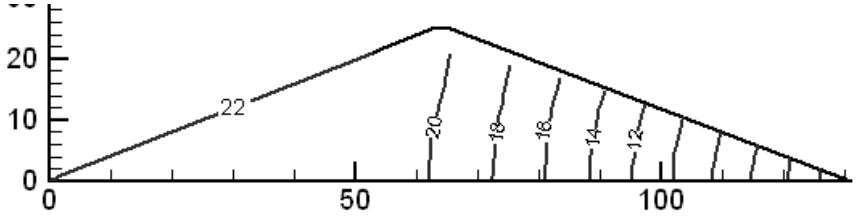

Fig.15. Equipotentials in homogenous earthfill dam

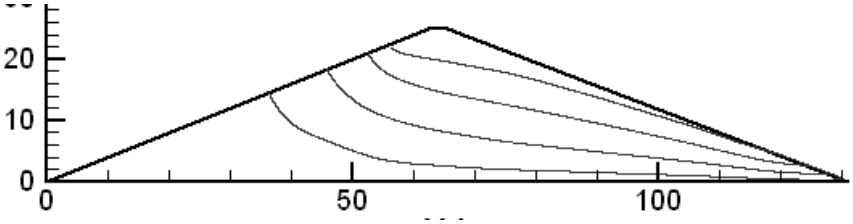

Fig.16. flow (stream)lines in homogenous earthfill dam

define Γ_2. The nodal potentials on Γ_2 and Γ_3 are then used to modify the position of the free surface, and the new problem is solved again. This procedure is continued until convergence is achieved. Figure (14) illustrates the convergence of Γ_2 and Γ_3 boundaries to their final positions.

Equipotentials and flow lines are presented in figures (15) and (16) respectively.

Conclusion

A truly meshless method, discrete least

square method (DLSM) is presented in this paper. The problem domain would be discretized by some nodes then using MLS shape function with a least square technique a symmetric stiffness matrix is constructed. Results of numerical examples show a good approximation for both regular and irregular nodes positioning. Increasing of nodes will cause better approximations. And the important characteristic of this method is that, dose not need any background mesh for integration.

References

[1] Gingold RA, Moraghan JJ. Smoothed particle hydrodynamics: theory and applications to non-spherical stars. Monthly Notices of the Royal Astronomical Society 1977; 181:375–389.

[2] Belytschko T, LuY, GuL. Element free Galerkin methods. International Journal for Numerical Methods in Engineering 1994; 37:229–256

[3] Belytschko T, Krongauz Y, Organ D et al. Meshless methods: An overview and recent developments. Computer Methods in Applied Mechanics and Engineering 1996; 139:3–47.

[4] Liu WK, Jun S, Zhang YF. Reproducing kernel particle methods. International Journal for Numerical Methods in Fluids 1995; 20:1081–1106.

[5] O˜nate E, Idelsohn S, Zienkiewicz OC, Taylor RL. A 1nite point method in computational mechanics. Applications to convective transport and Uuid Uow. International Journal for Numerical Methods in Engineering 1996; 39(22):3839–3866.

[6] Liszka TJ, Duarte CAM, Tworzydlo WW. hp-meshless cloud method. Computer Methods in Applied Mechanics and Engineering 1996; 139:263 –288.

[7] Atluri SN, Zhu TL. The meshless local Petrov–Galerkin (MLPG) approach for solving problems in elasto-statics. Computational Mechanics 2000; 25:169 –179.

[8] Atluri SN, Zhu TL. New concepts in meshless methods. International Journal for Numerical Methods in Engineering 2000; 47(1–3):537–556.

[9] Atluri SN, Kim HG et al. A critical assessment of the truly meshless local Petrov–Galerkin (MLPG), and local boundary integral equation (LBIE) methods. Computational Mechanics 1999; 24:348 –372.

[10] Atluri SN, Zhu T. A new meshless local Petrov–Galerkin (MLPG) approach in computational mechanics. Computational Mechanics 1998; 22:117–127.

[11] Atluri SN, Sladek J et al. The local boundary integral equation (LBIE) and it's meshless implementation for linear elasticity. Computational Mechanics 2000; 25:180 –198.

[12] Zhu T, Zhang JD, Atluri SN. A local boundary integral equation (LBIE)

method in computational mechanics, and a meshless discretization approach. Computational Mechanics 1998; 21:223 –235.

[13] Zhang X, Liu XH, Song KZ, Lu MW. Least-squares collocation meshless method. International journal of numerical methods in engineering 2001; 51:1089-1100.

[14] Wang QX, Li H, Lam KY. development of a new meshless – point weighted least –squares (PWLS) method for computational mechanics. . Computational Mechanics 2005; 35:170 –181.